analytical chemistry

pubs.acs.org/ac

Article

Determination of the Distance Between the Cytochrome and Dehydrogenase Domains of Immobilized Cellobiose Dehydrogenase by Using Surface Plasmon Resonance with a Center of Mass Based Model

Jani Tuoriniemi, Lo Gorton, Roland Ludwig, and Gulnara Safina*

Cite This: *Anal. Chem.* 2020, 92, 2620–2627

Read Online

ACCESS | Metrics & More | Article Recommendations

ABSTRACT: Changes in the tertiary conformation of adsorbed biomolecules can induce detectable shifts ($\Delta\theta_r$) in the surface plasmon resonance (SPR) angle. Here it is shown how to calculate the corresponding shifts in the adsorbate's center of mass (Δz_{avg}) along the sensing surface normal from the measured $\Delta\theta_r$. The novel developed model was used for determining the mean distance between the cytochrome (CYT) and flavodehydrogenase (DH) domains of the enzyme cellobiose dehydrogenase (CDH) isolated from the fungi *Neurospora crassa*, *Corynascus thermophilus*, and *Myriococcum thermophilum* as a function of pH, [Ca^{2+}], and substrate concentration. SPR confirmed the results from earlier electrochemical and SAXS studies stating that the closed conformation, where the two domains are in close vicinity, is stabilized by a lower pH and an increased [Ca^{2+}]. Interestingly, an increasing substrate concentration in the absence of any electron acceptors stabilizes the open conformation as the electrostatic repulsion due to the reaped electrons pushes the DH and CYT domains apart. The accuracy of distance determination was limited mostly by the random fluctuations between replicate measurements, and it was possible to detect movements <1 nm of the domains with respect to each other. The results agreed with calculations using already established models treating conformational changes as contraction or expansion of the thickness of the adsorbate layer ($t_{protein}$). Although the models yielded equivalent results, in this case, the Δz_{avg}-based method also works in situations, where the adsorbate's mass is not evenly distributed within the layer.

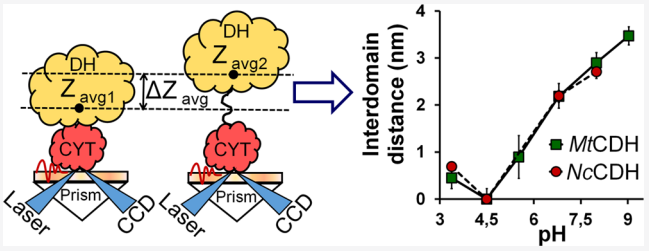

Surface plasmon resonance[1,2] (SPR) can be used to measure the refractive index (n) of layers of immobilized biomolecules with a sufficient sensitivity to detect changes in the tertiary conformation of immobilized protein molecules. Since the pioneering studies demonstrating the possibility of detecting structural changes in cytochrome *c* upon oxidation and reduction,[3] and denaturation of dihydrofolate reductase from *E. coli* at low pH,[4] the field has progressed to more application oriented work.

On one hand, conformational changes contributing to the SPR signal can limit the accuracy in conventional biosensing. On the other hand, they allow the use of receptors that alter their conformation upon ligand binding to quantify low molecular weight compounds, for which the sensitivity would otherwise be too low.[5] It has been demonstrated that despite the increase in mass, binding of maltose to maltose-binding protein results in a negative resonance angle (θ_r) shift ($\Delta\theta_r$).[5] The same study also showed that quantification of Na^+ and Ca^{2+} is possible owing to the signal arising from conformational changes in immobilized tissue transglutaminase upon binding of these ions. Later, a sensor detecting Ca^{2+} at concentrations as low as 23 μM was designed based on the localized SPR phenomenon in nanostructured Ag layers and conformational changes in calmodulin.[6] SPR has provided a wealth of information on the conformational dynamics of calmodulin and other Ca^{2+} binding proteins.[7,8]

Other surface sensitive techniques developed for conformational analysis include coupled plasmon waveguide resonance,[9] that is SPR where additional information is extracted from optically anisotropic layers by measuring the reflectance curve separately for the *s* and *p* polarization directions, dual beam interferometry[10] that measures changes in the thickness of the adsorbate layer ($t_{protein}$) with a higher sensitivity than ellipsometry and quartz crystal microbalance,[11] where the viscosity dependent rate of energy dissipation can be related to structural features.

Received: October 1, 2019
Accepted: January 9, 2020
Published: January 9, 2020

https://dx.doi.org/10.1021/acs.analchem.9b04490
Anal. Chem. 2020, 92, 2620–2627

Detailed studies of conformational changes that go beyond detecting their occurrence require quantitative models that relate the $\Delta\theta_r$ to specific changes in the molecular structure. So far models have assumed that the immobilized proteins form a layer that has a thickness, $t_{protein}$, and hold a volume fraction, $f_{protein}$, of adsorbed biomolecules.[3,12] It is possible to calculate the refractive index for the protein layer ($n_{protein}$) for a such system as a function of $f_{protein}$ by the Lorentz−Lorenz equation.[12] The conformational changes are thought to either expand or contract $t_{protein}$. A contraction increases $f_{protein}$ and, therefore, $n_{protein}$. The effective n as it is measured by SPR for the whole sample (n_{eff_sample}) is calculated by integrating the refractive index weighted by the evanescent field intensity as a function of the distance from the sensing surface.

A drawback of such models is that, unless the adsorbate mass is evenly distributed within the layer, the $t_{protein}$ and $n_{protein}$ become mere mathematical parameters that are difficult to relate directly to any changes in molecular structure. This article presents an alternative data analysis method of calculating the shift (Δz_{avg}) in the adsorbate center of mass (z_{avg}) along the sensor surface normal. The approach is used for determining the distance between the two domains of three different cellobiose dehydrogenases (CDH) with nm precision as a function of pH, [Ca^{2+}], and substrate concentration.

CDHs[13,14] are sugar oxidizing enzymes that have been isolated and characterized from numerous fungal species of both the phyla of *Basidiomycota* and *Ascomycota*. CDHs from basidiomycete fungi have a strong preference to oxidize cellobiose, cello-oligosaccharides, and lactose, while the ones isolated from ascomycete tend to be more promiscuous regarding their substrates also converting malto-oligosaccharides and monosaccharides such as glucose. CDH consists of two separate domains connected by a flexible polypeptide linker of variable length (between 15 to 35 amino acids). The larger, flavodehydrogenase (DH) domain, contains the active site and one FAD cofactor, the smaller cytochrome (CYT) domain contains a *b*-type heme as cofactor.

In the catalytic reaction FAD takes up two electrons from the substrate and transforms into its fully reduced state, $FADH_2$. In the reoxidation reaction electrons are subsequently transferred one at a time from the $FADH_2$ to the heme *b* to facilitate the direct electron transfer (DET) to large molecular one electron acceptors like lytic polysaccharide monooxygenase, cytochrome *c* or electrodes.[13,14] The domains in CDH can alter between a closed conformation, where the domains are locked in a position that brings the two prosthetic groups into proximity for fast and effective electron transfer, or an open one, where the domains are mobile within the constraints set by the linker.[15,16] The existence of two conformational states in solution has been confirmed by small-angle X-ray scattering (SAXS) for CDH isolated from the ascomycete fungi *Myriococcum thermophilum* (*Mt*CDH) and *Neurospora crassa* (*Nc*CDH), and the structure of both the open and closed conformations have been determined by X-ray crystallography.[17] The presence and exchange between the two conformational states has also been demonstrated by small angle neutron scattering (SANS)[18] and atomic force microscopy.[19]

The preferred conformation is probably mainly dependent on the electrostatic repulsion or attraction between the domains.[20] The so far identified factors stabilizing the closed conformation are lower pH and increasing concentrations of divalent metal ions.[15,16] The interaction between the two domains is crucial for the functioning of enzyme electrode devices, because the electrons can only under very special conditions be transferred directly from the DH to the electrode, the most common pathway to the surface being via the CYT.[21] Surface-immobilized CDH is used in enzyme electrode devices such as amperometric saccharide sensors[22] and biofuel cells.[23] The function of CDH in such applications is to oxidize analyte or fuel and transfer the electrons to the electrode surface.A promising CDH based lactose sensor has been evaluated for monitoring the discharge levels in the wastewater stream of a dairy plant[24] and is now commercialized by the company DirectSens (http://www.directsens.com). Biofuel cells based on enzymes, such as CDH, could become important when the ever-decreasing size of electronic devices start to demand power sources with a comparable potential for miniaturization.

The two domains of CDH can be modeled as spheres having certain molecular masses with the distance ($d_{CYT\text{-}DH}$) between them varying as a function of the chemical environment. It will be shown how to calculate the $d_{CYT\text{-}DH}$ from the measured $\Delta\theta_r$ via Δz_{avg}. SPR can, owing to its sensitivity, acquire more detailed information about the chemical parameters influencing the interaction between the two domains than what was possible in the earlier electrochemical and SAXS-based studies. It was also possible to investigate the role of the substrate, which is otherwise difficult to gauge by electrochemical methods measuring the differences between the reduction rates for DET and mediated electron transfer (MET).

EXPERIMENTAL SECTION

Chemicals and Reagents. Cellobiose dehydrogenases (CDH) from *Neurospora crassa* (*Nc*CDH, specific activity 8.54 U mg^{-1}, protein concentration 9 mg mL^{-1}), *Corynascus thermophilus* (*Ct*CDH, syn. *Crassicarpon thermophilum*, specific activity 5.9 U mg^{-1}, protein concentration 7 mg mL^{-1}), CDH holoenzyme from *Myriococcum thermophilum* (*Mt*CDH, syn. *Crassicarpon hotsonii*, specific activity 3.1 U mg^{-1}, protein concentration 7.3 mg mL^{-1}), and its isolated dehydrogenase domain (*Mt*DH, amino acids 251−828, protein concentration 6.4 mg mL^{-1}) were recombinantly produced by expression in *Pichia pastoris*,[25] and isolated and purified according to the protocol described in Harreither et al.[26] The enzyme solutions were stored in a 50 mM acetate buffer (pH 5.5 at 4 °C).

A fresh 0.1 M stock solution of *β*-lactose (Sigma-Aldrich, Stockholm, Sweden) was prepared and stored overnight to reach mutarotational equilibrium. 11-Mercaptoundecanoic acid (11-MUA), *N*-ethyl-*N*′-dimethylaminopropyl carbodiimide (EDC), *N*-hydroxysuccinimide (NHS), ethanolamine hydrochloride, NH_3, and H_2O_2 were purchased from Sigma-Aldrich (Stockholm, Sweden).

The acetate-based working buffers were prepared from 0.05 M sodium acetate (Merck International AB, Stockholm, Sweden) and titrated with acetic acid solution (Sigma-Aldrich) to obtain pH values ranging from 3.4 to 6.8. Tris-(hydroxymethyl) aminomethane (Tris) and HCl (both from Merck International AB, Stockholm, Sweden) were used to prepare the buffers with pH values from 7.5 to 9.0. $CaCl_2$ and lactose were added to the buffers at concentrations up to 100 mM in some experiments.

The buffers and lactose solutions were filtered through 0.2 *μ*m Whatman syringe filters (Sigma-Aldrich, St. Louis, MO) and degassed for 20 min prior to measurements. All reagents

https://dx.doi.org/10.1021/acs.analchem.9b04490
Anal. Chem. 2020, 92, 2620−2627

used were of analytical grade. All the solutions were prepared using Milli-Q water (18.2 MΩ cm, Millipore, Billerica, MA).

SPR Instrument and Measurements. The measurements were conducted using a dual channel SPR Esprit instrument (Metrohm Autolab, Utrecht, The Netherlands). Detailed description of the device and experimental setup can be found in www.ecochemie.nl/download/Manuals/ESPRIT_user_manual_4.4.0-2.pdf. The Au-coated slides (25 mm Ø) were provided by the instrument manufacturer. The samples and solutions were introduced manually to the measurement chamber using a micropipette. Temperature was continuously monitored during the measurements and was 22 ± 1 °C. It was deemed that temperature fluctuations did not have any significant influence on the results. The used wavelength was 670 nm. Data was acquired using Autolab software (version 4.4) integrated with the analyzer. All measurements were conducted on freshly modified surfaces. After the SPR responses of the test solutions were recorded, the channels were rinsed with working buffer. Where applicable, the injections were performed in order of increasing concentrations.

Preparation of the SPR Slides. The gold slides were cleaned by boiling them during 10 min in a mixture of 35% NH_3, 33% H_2O_2, and Milli-Q water (v/v 1:1:5). The slides were rinsed with Milli-Q water and ethanol, and were immediately immersed into a 1 mM 11-MUA alcohol solution. The slides were kept in a dark place at room temperature for 16−24 h for stabilizing the formed thiol monolayers. Prior to mounting into the SPR analyzer, the slides were thoroughly rinsed with ethanol and Milli-Q water to remove any loosely attached thiols, and dried in a stream of N_2.

Enzyme Immobilization. CDHs were immobilized on the thiol functionalized Au surface via amine coupling. A total of 50 μL of a freshly prepared mixture of aqueous solutions of 0.4 M EDC and 0.1 M NHS (v/v 1:1) was applied on both SPR channels for 10 min. Then, 50 μL of enzyme solution diluted with acetate buffer (pH 5, v/v 1:1) was applied to one of the channels for 15−30 min, while the other was filled with acetate buffer to leave it as a reference channel. When the SPR signal due to binding of CDH to the EDC/NHS activated surface ceased to increase and reached a plateau, the excess of the physically adsorbed enzyme was removed by rinsing the channel with acetate buffer. When the amine coupling immobilization scheme is applied, the enzyme is anchored to the thiol-modified Au surface by its *N*-terminus,[27] which is located at the CYT domain.[28] This specificity is because the *N*-terminus reacts faster than other CDH surface exposed amine groups, mainly lysine residues, as a larger fraction of them are due to their higher pK_a values protonated at pH 5 and therefore will not react.[27] The unoccupied sites were blocked by applying a 1 M ethanolamine hydrochloride solution (pH 8.5) for 10 min, after which it was rinsed away by ample amounts of acetate buffer. The reference channel also underwent the deactivation step with ethanolamine hydrochloride.

Electrochemical Measurements. Cyclic voltammetry (CV) was performed in the electrochemical cell of the SPR instrument, where the enzyme modified gold surface was used as the working electrode. A Pt wire was used as counter electrode and a miniature Ag|AgCl electrode provided by the instrument manufacturer as the reference. The electrodes were connected to a three-electrode potentiostat (Metrohm Autolab, Utrecht, The Netherlands). CVs were recorded between −0.15 to 0.35 V at scan rate 0.01 V s^{-1}.

THEORY

This section first recapitulates the measurement principles of SPR and then develops the theory for calculating the Δz_{avg}. Figure 1 illustrates the nature of CDH conformational changes and explains the terminology used in this work. For a more exhaustive description of the underlying theory of SPR phenomena, instrumentation and applications of SPR the reader is referred to, for example, Homola et al.[2] and Räther.[1]

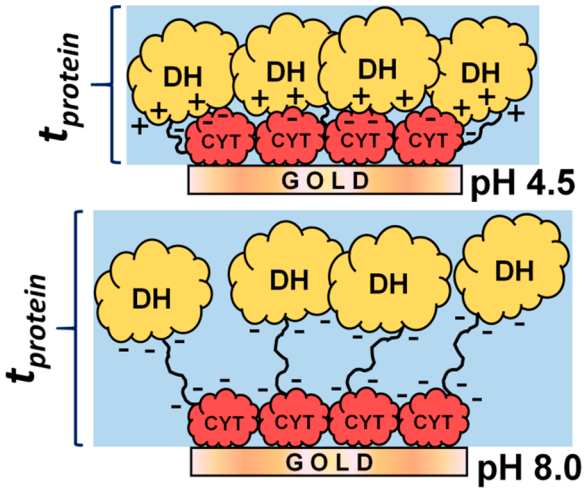

Figure 1. Schematic illustration of the pH dependent protein layer thickness ($t_{protein}$) of the closed (at pH 4.5) and open (at pH 8.0) conformations of the CDH molecules immobilized on the gold SPR slide. The $t_{protein}$ decreases and increases as a result of electrostatic attraction and repulsion of the oppositely (at pH 4.5) and equally (at pH 8.0) charged enzyme domains. The spacer molecule is not depicted for clarity of the figure. The buffer present within the $t_{protein}$ together with protein molecules is shown as a blue background.

Measuring the Refractive Index of Layered Samples. The effective refractive index (n_{eff_sample}) of the matter within the exponentially decaying evanescent field can be calculated from the θ_r using eq 2 in ref 29. This equation can be approximated by a linear relation between the θ_r and n_{eff_sample} for the relatively small resonance angle shifts that are produced by a protein layer adsorbed on the sensing surface. The samples that are measured in this work consist of three layers: (1) spacer molecule (11-MUA) attaching the CDH to the Au surface, (2) protein (more precisely protein+buffer; Figure 1), and (3) buffer on the top of the protein layer extending beyond the reach of the evanescent field. The n_{eff_sample} for such a layered sample is the evanescent field intensity weighted average of the n of the individual layers. It is calculated by integrating the n as a function of the distance from the surface (z) weighted by the exponentially decaying intensity of the evanescent field.[12]

$$n_{eff\_sample} = 2C\left(\int_0^{z_{spacer}} n_{spacer} e^{-2Cz} dz + \int_{z_{spacer}}^{z_{protein}} n_{protein} e^{-2Cz} dz + \int_{z_{protein}}^{\infty} n_{buffer} e^{-2Cz} dz\right) \quad (1)$$

https://dx.doi.org/10.1021/acs.analchem.9b04490
Anal. Chem. 2020, 92, 2620−2627

where n_{spacer}, $n_{protein}$, and n_{buffer} are the refractive indexes of 11-MUA, the protein+buffer composite layer, and the buffer, respectively.

The measured quantity in these experiments is the angle difference between the measurement channel containing the sample and a reference channel containing spacer and buffer layers only ($\Delta\theta_{r\_sample}$). For thin protein layers that only reach up to a small fraction of the extent of the evanescent field, it is valid to assume that the n_{buffer} containing term in eq 1 is equal regardless whether a protein layer is present or not. Also, calculations using the Lorentz−Lorenz equation show that the $n_{protein}$ is to a good approximation a linear function of the mass fraction of protein in the layer, and the integrated refractive index over the whole width of the protein layer containing a certain mass of protein is virtually invariant regardless of its thickness.

The $\Delta\theta_{r\_sample}$ can under these assumptions be written:

$$\Delta\theta_{r\_sample} \cong \int_{z_{spacer}}^{z_{protein}} (n_{protein} - n_{buffer}) e^{-2Cz} dz$$

$$= k m_{protein} (e^{-2Cz_{spacer}} - e^{-2Cz_{protein}}) \quad (2)$$

where $m_{protein}$ is the surface concentration of protein (ng mm^{-2}), and k is the sensitivity (°ng^{-1} mm^2). The $\Delta\theta_{r\_sample}$ for a given mass of adsorbed protein becomes thus an exponentially decreasing function of the layer thickness in this simple model that assumes that the protein mass is evenly distributed within the layer.

The value of the decay coefficient C was calculated by[1]

$$C = \left| \frac{\lambda}{2\pi} \left(\frac{m + n_{eff\_sample}^2}{n_{eff\_sample}^2} \right)^{0.5} \right|^{-1} \quad (3)$$

where λ is the wavelength (m) and m is the relative permittivity of Au ($-14.1269 + 1.0961i$ at λ = 670 nm, where $i = \sqrt{-1}$). C is 3.5×10^6 m^{-1} if it is assumed that the n_{eff_sample} is that of pure water. With such a decay rate, the intensity of illumination decreases to $1/e$ at a z of ∼142 nm. The n_{eff_sample}, including both the protein layer and the buffers used for testing the chemical parameters is higher than that for pure water. However, according to our calculations it is unlikely that the adsorbed protein and the used buffers would increase C by more than 3%. It was also shown by Liedberg et al.[30] in their calculations that the decay rate is not significantly affected by thin adsorbate layers.

Defining the *Q* Ratio. Being said that the n is linearly dependent on the θ_r and knowing that that the angle depends linearly on adsorbed protein mass (∼0.120° ng^{-1} mm^2[31]) and concentration of buffer components, the $\theta_{r\_sample} \approx \theta_{r\_H2O} + \theta_{r\_protein} + \theta_{r\_buffer}$. The used SPR instrument only measures the reflectance in a 4° wide range. Without calibration with a reference sample it is impossible to determine with sufficient certainty which incidence angle values this range includes. Therefore, after subtracting the buffer contribution from the reference channel, the angle that would be produced by pure water (θ_{r_H2O} = 69.55°) was added to the $\Delta\theta_{r\_sample}$ to form an estimate of the θ_{r_sample}, where the buffer contribution has been removed ($\theta_{r\_H2O} + \theta_{r\_protein}$). The data analysis in this work is based on the ratio Q between that of the protein layer exposed to the test buffer and a reference value obtained when exposed to a reference buffer arbitrarily chosen as a reference chemical state. The Q is thus defined as

$$Q = \frac{\Delta\theta_{r\_sample} + \theta_{r\_H_2O}}{\Delta\theta_{r\_ref\_buffer} + \theta_{r\_H_2O}} \quad (4)$$

By adding θ_{r_H2O} in eq 4, the Q becomes an approximation to the ratio of the n_{eff_sample} for the test buffer and the reference buffer corrected for the contribution of the different buffer components.

The next steps will be to relate the Q to the protein layer thickness ($t_{protein}$) and differences in the mean distance between the two enzyme domains.

***Q* as a Function of $t_{protein}$.** By calculating the $n_{protein}$ for different mass fractions of protein within the $t_{protein}$ using the Lorentz−Lorenz equation and substituting the values into eq 2, k was determined to be 0.122° ng^{-1} mm^2. This is close to the commonly accepted value of sensitivity for protein adsorption ∼0.120° ng^{-1} mm^2.[31] There is a weak, but still measurable, dependence on the $t_{protein}$. If, based on the crystallographic dimensions of CDH,[17] a thickness of 4.5 nm was chosen as a reference state, where Q = 1, then Q will depend on $t_{protein}$ in a close to linear (R^2 = 0.9996) relationship as $Q \cong 1.0215 - 0.0048 t_{protein}$ (Figure 2). Q thus increases, while $t_{protein}$ decreases, because the protein mass moves closer to the surface of the SPR slide, where it interacts with a stronger evanescent field.

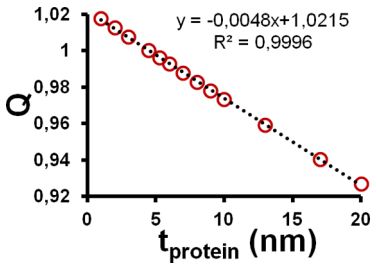

Figure 2. Q as a function of $t_{protein}$ of CDH.

***Q* as a Function of the Center of Mass of the Protein Layer.** The layer-based model assumes that the protein mass is evenly distributed within the layer. For a molecule such as CDH, for which the conformational changes consist of two domains with known masses moving with respect to each other, it is more useful to relate the measured values of Q to Δz_{avg} rather than to $t_{protein}$. If the masses of the domains are known, any change in $d_{CYT\text{-}DH}$ ($\Delta d_{CYT\text{-}DH}$) can be calculated from the resulting change in Δz_{avg} of the entire CDH molecule. An illustration clarifying the method that is presented below is shown in Figure 3. Equation 2 can be restated as $\Delta\theta_{r\_sample} = k m_{protein} I_{avg}$, where I_{avg} is the evanescent field intensity that the protein molecules are on average exposed to. The value of $m_{protein}$ remains constant upon conformational changes, while z_{avg}, and therefore, I_{avg} shifts. I_{avg} and z_{avg} are according to the formula of weighted averages related by

$$I_{avg} \frac{\int_{z_{spacer}}^{z_{protein}} (n_{protein}(z) - n_{buffer}) e^{-2Cz} dz}{\int_{z_{spacer}}^{z_{protein}} (n_{protein}(z) - n_{buffer}) dz} = e^{-2Cz_{avg}} \quad (5)$$

Note that $n_{protein}$ is now allowed to vary with z to account for the molecular structure. Because the integral of $n_{protein}$ over the whole layer only depends on the $k m_{protein}$, the denominator in eq 5 stays equal upon conformational changes. The I_{avg} for the whole sample is $I_{avg\_sample} = k m_{protein} I_{avg\_protein} + k_{buffer} I_{avg\_buffer}$. According to eqs 4 and 5, the Q ratio between the

https://dx.doi.org/10.1021/acs.analchem.9b04490
Anal. Chem. 2020, 92, 2620−2627

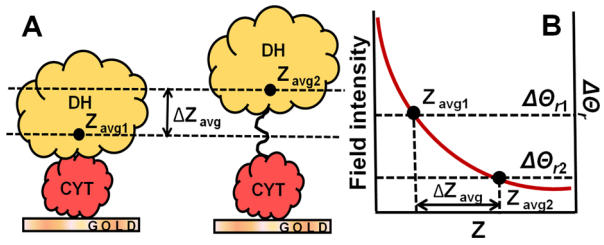

Figure 3. (A) Schematic illustration of the shift (Δz_{avg}) in the center of mass of CDH (depicted as a black dot) upon a change from closed (z_{avg1}) to open (z_{avg2}) conformation. (B) Curve showing the exponential decaying of field intensity as a function of z and $\Delta\theta_r$ as a function of z_{avg}. The resonance angle shift ($\Delta\theta_r$) decreases when the enzyme undergoes a conformational change from contracted state ($\Delta\theta_{r1}$) to expanded state ($\Delta\theta_{r2}$).

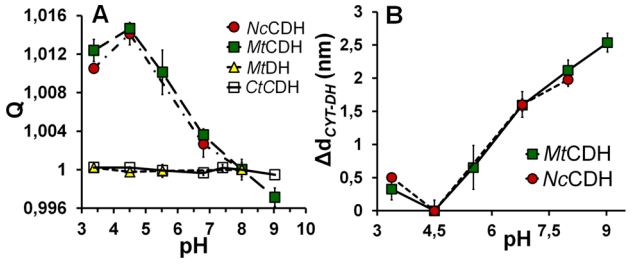

Figure 4. (A) Dependence of Q on pH measured for different holoenzymes and the isolated *Mt*DH domain. (B) The increase in the interdomain distance from its minimum value as a function of pH. The error bars denote 95% confidence intervals.

conformational states of the sample and the reference buffer therefore becomes

$$Q = \frac{\Delta\theta_{r\_sample} + \theta_{r\_H_2O}}{\Delta\theta_{r\_ref\_buffer} + \theta_{r\_H_2O}} = \frac{I_{avg_{sample}}}{I_{avg_{ref\_buffer}}} = e^{-2C\Delta z_{avg}} \quad (6)$$

where $\Delta z_{avg} = z_{avg\_sample} - z_{avg\_ref\_buffer}$.

Rearranging eq 6 gives

$$\frac{\ln(Q)}{-2C} = \Delta z_{avg} \quad (7)$$

The protein layers contribution to the Δz_{avg}, as defined by eq 5, is estimated by multiplying eq 7 by 0.73 to make the slope of Q as a function of Δz_{avg} (seemingly linear R^2 = 0.9999) to agree with that calculated in Figure 2. In the section below, eq 7 with this correction factor is used for calculating the interdomain distance, $d_{CYT\text{-}DH}$, in several CDH variants isolated from different fungi.

RESULTS AND DISCUSSION

Catalytic Activity of Immobilized CDH, Measured Using Electrochemical SPR. Cyclic voltammetry using the SPR slide as a working electrode and lactose as a substrate at pH 4.5 resulted in a linear relation (R^2 = 0.9999) between the concentration of lactose (10, 30, and 100 mM) and current measured at a potential of 0.25 mV versus AgIAgCl. This verified that CDH retains its activity and, therefore, native conformation upon immobilization.

A practical finding was that it was safer to simply place the reference electrode consisting of a thin Ag wire with a knob of AgCl at one end directly into the buffer laying on the SPR slide rather than to insert the electrode into its intended holder. Otherwise, the holder is in contact with the sample via a narrow channel, where air bubbles could easily form between the electrode and the sample, and the lost electrical contact could ruin measurements when the automatically controlled potentiostat spuriously applied high voltages that destroyed the enzyme.

pH-Dependent Conformational Changes in CDH. *Nc*CDH, *Ct*CDH, and *Mt*CDH were immobilized on the sensor slides and repeatedly exposed to a series of buffers with different pH values. The surface concentration of adsorbed CDH was at least 10 ng mm^{-2} judging from the $\Delta\theta_r$ of more than 1.220° for the sensor chips characterized in this Article. It was calculated that this corresponded to ~85% of a close packed monolayer coverage of the surface with the enzyme. The Q values as a function of pH are shown in Figure 4A. They were calculated with the buffer having a pH 8 arbitrary chosen as the reference buffer. The random scatter in Q values measured for each pH fell in a relatively narrow range for all enzymes. No drift was observed during repeated cycling through the pH values. For *Nc*CDH and *Mt*CDH, there is a pronounced maximum in Q around pH 4.5, while it is practically invariant for *Ct*CDH and *Mt*DH.

Both *Nc*CDH and *Mt*CDH are known to reach a DET maximum when the pH is reduced from ~9 to ~4.5.[16] This is explained by the fact that the enzymes assume a predominantly closed conformation facilitating electron transfer between the two domains. This would contract the enzyme layer decreasing z_{avg} (Figure 3), and accordingly, Q in Figure 4A increases.

To ascertain that the shifts in Q were related to the interaction between the two domains, a control experiment was made with a fragment containing only the isolated dehydrogenase domain from *Mt*DH. No conformational changes could be observed despite that the remaining DH comprises most of the enzyme mass (>70%;[26] Figure 4A). The shifts in Q therefore add to the body of evidence for that the two domains are at high pH predominantly not attached to each other.

There were no conformational changes observed for *Ct*CDH (Figure 4A). For this enzyme, the reported DET activity maxima at pH ~ 6 coincides with that of the MET rate of the dehydrogenation reaction catalyzed by the DH domain.[16] The SPR thus corroborates these earlier electrochemical results that suggest that for this enzyme the closed conformation predominates at all pH values. This could be true also for other CDHs having high pH maxima of DET.

It is necessary to ascertain that the Q values were measured accurately enough before attempting to calculate the Δz_{avg} and the $d_{CYT\text{-}DH}$ values. There were no significant $\Delta\theta_r$ observed due to temperature differences upon changing the buffers. The value of θ_r is slightly distorted from the value predicted by eq 1 by factors such as surface roughness and density of impurities and microdefects such as cracks and pits on the Au layer that increase the imaginary part of the Au refractive index. The presence of defects on pristine sensor surfaces was confirmed by optical microscopy. The magnitude of this spurious contribution varies between different locations on the sensor surface. Therefore, a bias (δ) is introduced to $\Delta\theta_r$ by the referencing procedure (eq 4), where the sample and reference channels have different populations of defects. The resulting error (ε) in Q is likely to be given by

$$\frac{\Delta\theta_{r\_sample} + \theta_{r\_H_2O} + \delta}{\Delta\theta_{r\_ref\_buffer} + \theta_{r\_H_2O} + \delta} = Q + \varepsilon \quad (8)$$

https://dx.doi.org/10.1021/acs.analchem.9b04490
Anal. Chem. 2020, 92, 2620−2627

Tests where buffer from an identical preparation was applied to both measurement channels of the SPR instrument multiple times, changing the location of the measurement spot both by rotating and sometimes changing the slide, showed that δ was on average only ~0.06% of the resonance angle. Even if the Q values are close to unity, the roughness of the sensor surfaces is not enough to introduce significant errors into the data presented here. Rather, the accuracy in these measurements is determined by the random variation in Q when repeatedly applying the same buffer. It was typically ~0.05−0.1% RSD and probably arises from small changes in the structure of the delicate enzyme layer.

To calculate the mean interdomain distance ($d_{CYT\text{-}DH}$) from the Δz_{avg} one must remember that the CYT domain is anchored to the spacer-modified Au surface, while the DH domain is mobile in the open conformation. By using the equation for calculating the center of mass for a two-body system it can be shown that the shift of the interdomain distance, $\Delta d_{CYT\text{-}DH}$, is given by

$$\Delta d_{CYT-DH} = \frac{M_{CDH}}{M_{DH}} 0.73 \Delta z_{avg} \quad (9)$$

where M_{CDH} and M_{DH} are the molecular weights of the holoenzyme and DH domains, respectively. The values for M_{CDH} for *Mt*CDH[26] and *Nc*CDH[25] are 95 and 88 kDa, respectively, and the corresponding values for M_{DH} are 68 and 65 kDa.

The mean distances between the domains estimated by eqs 7 and 9 are shown in Figure 3B. Here it was assumed that the domains were in contact at the Q maxima at pH 4.5, that is, $d_{CYT\text{-}DH}$ = 0 (Figure 4B).

Figure 4B shows that $d_{CYT\text{-}DH}$ increases continuously for both enzymes as pH elevates from 4.5 to 9.0. This is explained by an augmenting negative net charge on both the CYT and DH domains (pH > pI), resulting in their stronger mutual repulsion. This finding is in agreement with the results of Bodenheimer et al.,[18,32,33] where modeling SANS and SAXS measurements suggested that, for *Nc*CDH, an increase in pH decreases the attraction between the equally charged CYT and DH domains, which causes the opening of the enzyme. For *Mt*CDH, the range, where the domains are in closest contact, coincides with that between the isoelectric points of the domains (calculated values CYT, pI 4.0, and DH, pI 4.5,[16] measured values 3.3 and 3.9[26]). That the prevalence of the closed conformation co-occurs with the oppositely charged domains is probably true for *Nc*CDH as well. For *Ct*CDH, this range is wider and located at higher pH values (CYT, pI 5.0 and DH, pI 6.2[16]), though, the domains stay bound to each other, even at relatively high pH values. The slight increase in $d_{CYT\text{-}DH}$ when lowering the pH from 4.5 to 3.4 is explained by the mutual repulsion of the now positively charged domains (pH < pI). Interestingly, contrary to the results here, no conformational changes for *Mt*CDH were detected with SAXS upon a shift of pH from the OEA optimum of 5.5 to 7.5.[16] The results in Figure 4B suggest that the domains are at high pH values separated by a gap of up to 2.5 nm, which is too wide for the electrons to tunnel through. This expectation is supported by the electrochemical observations.[16,34]

Ca^{2+}-Dependent Conformational Changes in CDH. The DET of CDH has been found to increase as a function of the concentration of divalent metal ions until a saturation level, or an optimum was reached at concentrations of a few tens of mM.[16] It was therefore investigated whether the $[Ca^{2+}]$ added to the tested buffers influences the binding of the two domains at several different pH values. The investigations were carried out for *Nc*CDH, *Mt*CDH, and the isolated *Mt*DH domain (Figure 5). The Q values were calculated using the $[Ca^{2+}]$ = 0 mM as a reference buffer.

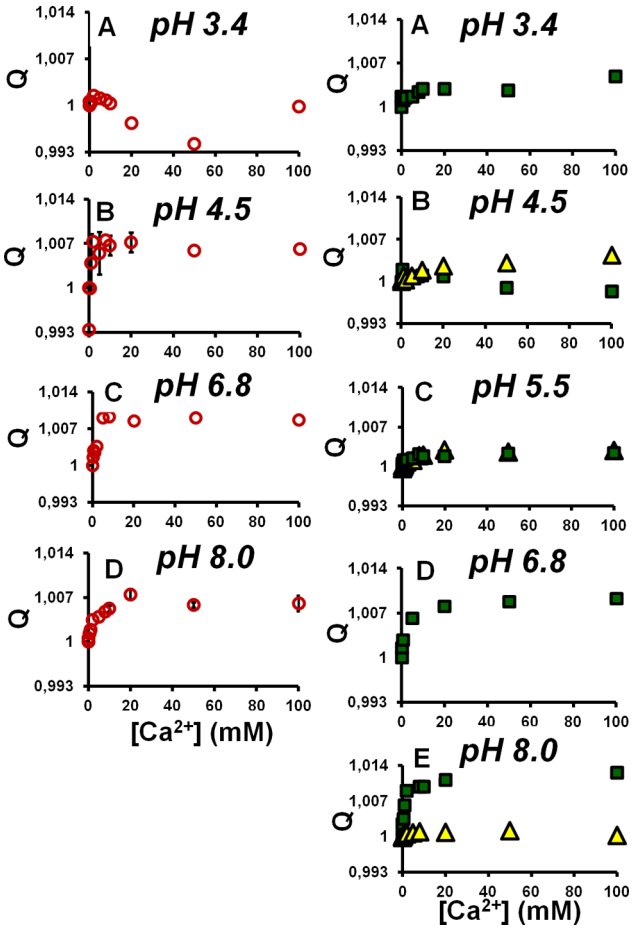

Figure 5. (Left panel, A−D) Dependence of the Q on $[Ca^{2+}]$ measured for *Nc*CDH at different pHs. (Right panel, A−E) Dependence of the Q on $[Ca^{2+}]$ measured for *Mt*CDH (green squares) and *Mt*DH (yellow triangles) at different pHs. The error bars denote 95% confidence intervals.

Except for the most acidic pH tried (3.4), Q tends to increase with the $[Ca^{2+}]$ (Figure 5, left panel). At pH 3.4 (Figure 5A, left panel), both domains of *Nc*CDH bear net positive charge and repulse each other. Binding of metal cations to the enzyme might further push the domains apart. At pH values of 4.5−8.0, addition of Ca^{2+} decreases the repulsion up to a concentration of ~5 mM, as it probably neutralizes any net negative charge on the domain and acts as a binding bridge between the CYT and DH domains. Further increasing the $[Ca^{2+}]$ does not substantially increase Q, as all available binding sites are probably already occupied (Figure 5B−D, left panel).

For *Mt*CDH, the Q profiles at different pHs were similar (Figure 5, right panel). The small changes in Q at pH 4.5−5.5 (Figure 5B,C, right panel) are most likely due to the fact that Ca^{2+} has little additional effect when the oppositely charged domains are already in close contact with each other. At the most acidic, pH 3.4, association of positive Ca^{2+} ions to the

https://dx.doi.org/10.1021/acs.analchem.9b04490
Anal. Chem. 2020, 92, 2620−2627

positively charged domains might as for *Nc*CDH additionally increase their repulsion (Figure 5A, right panel), and in contrast, at higher pHs (6.8−8.0), the DH domain is brought closer to the sensing surface being bridged by the divalent cation (Figure 5D,E, right panel). The shifts in *Q* for the isolated DH domain from *Mt*CDH were considerably smaller, which again confirms that the SPR shifts are mostly related to the separation between the domains (Figure 5B,C,E, right panel).

Ca^{2+} thus stabilizes the closed conformation. The calculated reduction in $d_{CYT\text{-}DH}$ ($-\Delta d_{CYT\text{-}DH}$) brought by 100 mM Ca^{2+} is shown as a function of pH in Figure 6 for both enzyme

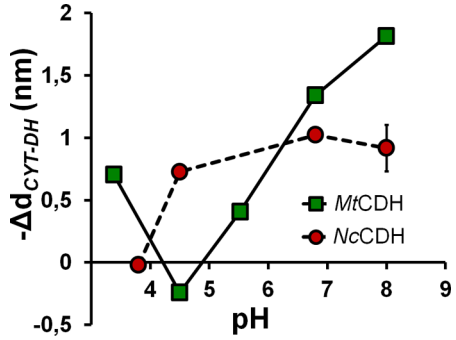

Figure 6. Decrease in the interdomain distance brought by 100 mM Ca^{2+} measured at different pHs for *Mt*CDH and *Nc*CDH. The error bar denotes 95% confidence interval.

variants. That the effect of Ca^{2+} becomes stronger with increasing pH values for *Mt*CDH is because the domains are further apart in the absence of added cations. Adding Ca^{2+} has no effect at pH 4.5 because the domains are already in nearly full contact. For *Nc*CDH, the effect of Ca^{2+} is strongest at the intermediate pH values (4.5 and 6.8) and never becomes as pronounced as for the former enzyme. It is therefore likely that Ca^{2+} is not binding as strongly to *Nc*CDH as to *Mt*CDH. Our SPR results corroborate the SAXS data, showing that the conformation of *Nc*CDH is pH-dependent, but affected by [Ca^{2+}] less than *Mt*CDH that undergoes substantial structural rearrangements in the presence of Ca^{2+}.[32]

Rotting wood is an acidic environment, where the [Ca^{2+}]concentrations in the saturation regions of Figure 5 can be found. It is therefore likely that in their natural environment CDHs from rot fungi are exposed to conditions favoring the closed conformation. A significant fraction of the charge of the DH domain is held by patches of acidic side chains of amino acids on the enzyme surface.[17] The locked conformation is probably favored for a wider range of conditions for ascomycete CDH because the density of acidic residues in these regions tends to be lower.

Lactose-Dependent Conformational Changes. The influence of lactose on the $\Delta d_{CYT\text{-}DH}$ was investigated for *Nc*CDH at pH 4.5 and 8.0 (Figure 7). Lactose was chosen as a substrate in these experiments because it is of general interest for biosensor applications.[24,35] It seems that the domains are pushed almost 1 nm apart by increasing the lactose concentration. This effect is more pronounced at high pH, where the domains are more loosely attached to begin with. There were no electron acceptors, except for the low concentration of dissolved oxygen incidentally present in the degassed buffer. Therefore, electrons harvested during the enzymatic oxidation of lactose to lactone can only leave the

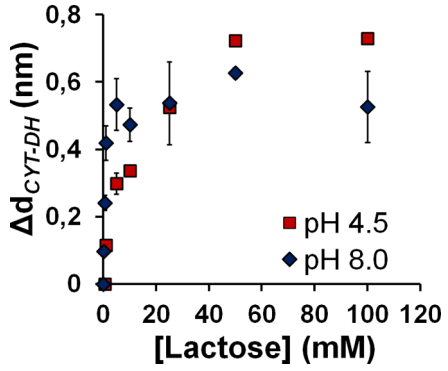

Figure 7. Effect of lactose on the interdomain distance measured at pH 4.5 and 8.0 for *Nc*CDH. The error bars denote 95% confidence intervals.

CDH very slowly, and both cofactors remain in the reduced state, which stabilizes the open conformation. The SPR results agree with the small-angle neutron scattering data that showed that the enzyme becomes more flexible at higher concentrations of substrate.[32] Such a feature might also have given an evolutionary advantage, because an increasing mobility of the CYT is likely to expedite electron transfer to its natural electron acceptor, lytic polysaccharide monooxygenase.

CONCLUSION

The sensitivity of SPR allows detecting most structural changes in a sample. However, quantitative interpretation is like for SAXS, dependent on the assumptions made for modeling the data. Developing new models for SPR data analysis is therefore the prime vehicle for conquering new areas of application. For instance, the authors have in earlier publications used coherent scattering theory that gives the effective refractive index of particle dispersions for extracting the concentrations and mean diameters of colloidal polystyrene particles.[29] This approach was later used for measuring the frequency of neurotransmitter exocytosis events from PC12 cells cultured on the SPR surface.[36]

It was here demonstrated that interpreting SPR angle shifts upon altering the chemical environment as changes in the distance between the two CDH domains gave results that are in accordance and complement earlier electrochemical and SAXS-based studies. It was possible to detect subnanometer movements of the domains with respect to each other, and it was shown how electrons reaped from the substrate push the two domains apart as they both become negatively charged.

SPR is a more accessible alternative to SAXS for immobilized protein characterization, as it only requires widely available benchtop equipment, with no need to be admitted to synchrotron facilities.

AUTHOR INFORMATION

Corresponding Author

Gulnara Safina − *University of Gothenburg, Gothenburg, Sweden, and Chalmers University of Technology, Gothenburg, Sweden;* orcid.org/0000-0003-0454-2694; Phone: +46737628613; Email: gulnara207@hotmail.com

https://dx.doi.org/10.1021/acs.analchem.9b04490
Anal. Chem. 2020, 92, 2620−2627

Other Authors

Jani Tuoriniemi − *University of Gothenburg, Gothenburg, Sweden*

Lo Gorton − *Lund University, Lund, Sweden;* orcid.org/0000-0002-7278-0478

Roland Ludwig − *BOKU − University of Natural Resources and Life Sciences, Vienna, Austria;* orcid.org/0000-0002-5058-5874

Complete contact information is available at: https://pubs.acs.org/10.1021/acs.analchem.9b04490

Notes

The authors declare no competing financial interest.

■ ACKNOWLEDGMENTS

The work has been supported by the Young Investigator Grant from the Swedish Research Council (Grant 621-2011-4395), the Olle Engkvist Byggmästare Foundation (Grant 2012/428), the Royal Swedish Academy of Sciences (Grant FOA12 V-111), the ÅForsk Foundation (Grant 11-360), the Foundation of Helge Ax:son Johnson, and the Foundation of Wilhelm and Martina Lundgren (Grant 2016-1403), the European Union's Horizon 2020 research and innovation program (ERC Consolidator Grant OXIDISE) under Grant Agreement No. 726396, and from the European Commission (Grant FP7-PEOPLE-2013-ITN-607793) and the Swedish Research Council (2014-5908).

■ REFERENCES

(1) Räther, H. *Surface Plasmons on Smooth and Rough Surfaces and on Gratings*; Springer: Berlin, Germany, 1988.

(2) Homola, J.; Yee, S. S.; Gauglitz, G. *Sens. Actuators, B* **1999**, *54*, 3−15.

(3) Boussaad, S.; Pean, J.; Tao, N. J. *Anal. Chem.* **2000**, *72*, 222−226.

(4) Sota, H.; Hasegawa, Y.; Iwakura, M. *Anal. Chem.* **1998**, *70*, 2019−2024.

(5) Gestwicki, J. E.; Hsieh, H. V.; Pitner, J. B. *Anal. Chem.* **2001**, *73*, 5732−5737.

(6) Hall, W. P.; Modica, J.; Anker, J.; Lin, Y.; Mrksich, M.; Van Duyne, R. P. *Nano Lett.* **2011**, *11*, 1098−1105.

(7) Dell'Orco, D.; Sulmann, S.; Linse, S.; Koch, K. W. *Anal. Chem.* **2012**, *84*, 2982−2989.

(8) Dell'Orco, D.; Koch, K. W. *ACS Chem. Biol.* **2016**, *11*, 2390−2397.

(9) Salamon, Z.; Brown, M. F.; Tollin, G. *Trends Biochem. Sci.* **1999**, *24*, 213−219.

(10) Cross, G. H.; Reeves, A. A.; Brand, S.; Popplewell, J. F.; Peel, L. L.; Swann, M. J.; Freeman, N. J. *Biosens. Bioelectron.* **2003**, *19*, 383−390.

(11) Milioni, D.; Tsortos, A.; Velez, M.; Gizeli, E. *Anal. Chem.* **2017**, *89*, 4198−4203.

(12) Jung, L. S.; Campbell, C. T.; Chinowsky, T. M.; Mar, M. N.; Yee, S. S. *Langmuir* **1998**, *14*, 5636−5648.

(13) Henriksson, G.; Johansson, G.; Pettersson, G. *J. Biotechnol.* **2000**, *78*, 93−113.

(14) Kracher, D.; Ludwig, R. *Bodenkultur* **2016**, *67*, 145−163.

(15) Ma, S.; Laurent, C. V. F. P.; Meneghello, M.; Tuoriniemi, J.; Oostenbrink, C.; Gorton, L.; Bartlett, P. N.; Ludwig, R. *ACS Catal.* **2019**, *9*, 7607−7615.

(16) Kracher, D.; Zahma, K.; Schulz, C.; Sygmund, C.; Gorton, L.; Ludwig, R. *FEBS J.* **2015**, *282*, 3136−3148.

(17) Tan, T. C.; Kracher, D.; Gandini, R.; Sygmund, C.; Kittl, R.; Haltrich, D.; Hällberg, B. M.; Ludwig, R.; Divne, C. *Nat. Commun.* **2015**, *6*, 7542−7552.

(18) Bodenheimer, A. M.; O'Dell, W. B.; Oliver, R. C.; Qian, S.; Stanley, C. B.; Meilleur, F. *Biochim. Biophys. Acta, Gen. Subj.* **2018**, *1862*, 1031−1039.

(19) Nakamura, A.; Tasaki, T.; Ishiwata, D.; Yamamoto, M.; Okuni, Y.; Visootsat, A.; Maximilien, M.; Noji, H.; Uchiyama, T.; Samejima, M.; Igarashi, K.; Iino, R. *J. Biol. Chem.* **2016**, *291*, 22404−22413.

(20) Kadek, A.; Kavan, D.; Felice, A. K. G.; Ludwig, R.; Halada, P.; Man, P. *FEBS Lett.* **2015**, *589*, 1194−1199.

(21) Schulz, C.; Kittl, R.; Ludwig, R.; Gorton, L. *ACS Catal.* **2016**, *6*, 555−563.

(22) Bollella, P.; Ludwig, R.; Gorton, L. *Appl. Materials Today* **2017**, *9*, 319−332.

(23) Scheiblbrandner, S.; Ludwig, R. *Bioelectrochemistry* **2020**, *131*, 107345.

(24) Glithero, N.; Clark, C.; Gorton, L.; Schuhmann, W.; Pasco, N. *Anal. Bioanal. Chem.* **2013**, *405*, 3791−3799.

(25) Sygmund, C.; Kracher, D.; Scheiblbrandner, S.; Zahma, K.; Felice, A. K. G.; Harreither, W.; Kittl, R.; Ludwig, R. *Appl. Environ. Microbiol.* **2012**, *78*, 6161−6171.

(26) Harreither, W. Cellobiose Dehydrogenase − an electrifying enzyme. Biochemical and electrochemical characterisation of cellobiose dehydrogenase for its application in biosensors and biofuel cells. *Ph.D. Thesis*, University of Natural Resources and Life Sciences: Vienna, 2010.

(27) Gedig, E. T. Surface Chemistry in SPR Technology. In *Handbook of Surface Plasmon Resonance*; Schasfoort, R. B. M., Tudos, A. J., Eds.; RSC Publishing: London, 2008; Ch. 6, pp 173−220.

(28) Hallberg, B. M.; Bergfors, T.; Bäckbro, K.; Pettersson, G.; Henriksson, G.; Divne, C. *Structure* **2000**, *8*, 79−88.

(29) Tuoriniemi, J.; Moreira, B.; Safina, G. *Langmuir* **2016**, *32*, 10632−10640.

(30) Liedberg, B.; Lundström, I.; Stenberg, E. *Sens. Actuators, B* **1993**, *11*, 63−72.

(31) Stenberg, E.; Persson, B.; Roos, H.; Urbaniczky, C. *J. Colloid Interface Sci.* **1991**, *143*, 513−526.

(32) Bodenheimer, A. M. Structural Characterization of the Fungal Cellulose Degrading Enzymes Cel7A and Cellobiose Dehydrogenase IIA. *Ph.D. Thesis*; North Carolina State University: Raleigh, NC, 2016.

(33) Bodenheimer, A. M.; O'Dell, W. B.; Stanley, C. B.; Meilleur, F. *Carbohydr. Res.* **2017**, *448*, 200−204.

(34) Harreither, W.; Sygmund, C.; Augustin, M.; Narciso, M.; Rabinovich, M. L.; Gorton, L.; Haltrich, D.; Ludwig, R. *Appl. Environ. Microbiol.* **2011**, *77*, 1804−1815.

(35) Safina, G.; Ludwig, R.; Gorton, L. *Electrochim. Acta* **2010**, *55*, 7690−7695.

(36) Moreira, B.; Tuoriniemi, J.; Kouchak Pour, N.; Mihalčíková, L.; Safina, G. *Anal. Chem.* **2017**, *89*, 3069−3077.